

1 Supplemental Methods for Traller et al “Genome and methylome of the oleaginous
2 diatom *Cyclotella cryptica* reveal genetic flexibility toward a high lipid phenotype”

3

4 *DNA extraction and purification*

5 Liquid cell cultures concentrated either by filtration using a 3.0µm polycarbonate
6 filter (DNA for genome sequencing) or by centrifugation in 50mL conical tubes at 4000
7 xg for 8 minutes (methylome DNA) using in an Eppendorf 5810R centrifuge. DNA for
8 genome and bisulfite sequencing was purified using CsCl as described in [1]. To remove
9 RNA contamination, DNA for bisulfite sequencing was treated with 10mg/mL stock of
10 RNase A for 15 minutes at 37°C.

11

12 *Genome Library Construction and Sequencing*

13 Three libraries were prepared following Illumina’s standard genomic DNA paired end
14 construction: “PE-short” (post-assembly empirical insert lengths ~90-235 nucleotides (nt)
15 exclusive of adapters [preparation target 180-230 nt], with mode 123 nt), “PE-medium”
16 (~155-330 nt [preparation target 230- 330 nt], mode 221 nt), and “PE-long” (~225-460 nt
17 [preparation target 330-430 nt] with mode 305 nt) for ~58% of inserts, with the balance
18 in a second mode ~60-225 nt peaking at ~105 nt). These were sequenced as paired end
19 76-mer + 76-mer reads on an Illumina GA-IIx 120-tiles/lane run (“TP003”) at the UCLA
20 BSCRC Core Sequencing facility, using two dedicated lanes for each of PE-short and PE-
21 medium, three dedicated lanes for PE-long, a dedicated PhiX control lane for RTA image
22 analysis autocalibration, and spiking in ≈1% Illumina PhiX into each non-control lane.
23 Two genomic DNA mate pair libraries (aiming for 10K nt effective inserts) were
24 prepared and run by Illumina service on a 48-tile/lane v3 HiSeq flow cell, each library on

25 a single dedicated lane: “MP-short” (effective ~2,100-3,320 nt with mode ~2,625 nt for
26 ~58% of inserts, with the balance in a PE-orientation [rather than MP-orientation] second
27 mode ~170-480 nt peaking at ~205 nt), and “MP-long” (~1,740-2,730 nt with mode
28 ~2,260 nt for ~63% of inserts, with the balance in a PE-oriented second mode ~176-535
29 nt peaking at ~223 nt). These were physically sequenced as paired end 101-mer + 10-mer
30 index + 101-mer, with the index reads and the last base of each main end discarded (in
31 the usual way so that the last retained base has bidirectional RTA phasing corrections).
32 The number of raw read pairs for PE-short/medium/long/control is found in Additional
33 File 1, Figure S1b. Only read pairs with no ‘N’ basecalls were retained; due to the pattern
34 of ‘N’ basecalls in PE-long, the first four bases of each end of its lanes were discarded
35 before this filter (and subsequent uses of this library).

36 The number of raw read pairs for MP-short and long libraries was 142,455,072 and
37 154,107,079, respectively, and only RTA PF=1-passing pairs were retained (Additional
38 File 1, Figure S1b). Although not used as a filter, relative to PF=1 read pairs, the ‘N’-free
39 read pairs for MP-short/long were ~98.9% / 98.6%.

40 The PE and MP libraries contributed ~23.4G nt and ~57.4G nt, respectively, for a
41 total of ~80.8G nt (≈ 461 x coverage of a 175Mbp genome; for 65-mers: ~3.4G and
42 ~20.7G, total ~24.0G and ≈ 137 x).

43 Using many iterations of a variety of standard and *ad hoc* assemblers and alignment
44 tools, with extensive inspection of intermediate stages and judgment calls made by hand,
45 read pairs from PE-short/medium/long and MP-short/long were used to construct high-
46 quality best assemblies from the available data for the chloroplast (“chrC”) and
47 mitochondrial (“chrM”) genomes in *C. cryptica*. In each case, a single complete circular

48 sequence of pure A/C/G/T's without gaps was formed (chrC 129,320 bp, chrM 58,021
49 bp). This was greatly assisted by the presence in NCBI of related genomes: KJ958480.1
50 for *Cyclotella* strain L04_2 chrC (~96% identity; also useful: KJ958481.1 for *Cyclotella*
51 strain WC03_2 chrC), and NC_007405.1 for *Thalassiosira pseudonana* chrM (more
52 distant; even on homologous stretches, overall percent identity ≈80%). The *C. cryptica*
53 chrM is estimated with 17,880 bp (~31%) being 120 exact copies of the 149 bp sequence
54 TTATCGGCCTCAAATCAAGCAGTGTTTAAGCTGGAAT
55 CTATCGGCCTCAAATCGAAACAGTGTTTTAGCCTGAAT
56 TTATCGGCCTCAAATCAAGCAGTGTTTAAGCTGGAAT
57 CTATCGGCCTCAAATCGAAACAGTGTTTTGCCTGAAT (which is itself four
58 approximate tandem copies of a smaller unit). Given current data, this region cannot be
59 completely resolved, and there is likely additional variation here, and the included
60 number of copies is an estimate informed in part by depth of coverage relative to other
61 chrM sequence.

62 The main genome assembly was performed with an ABySS 1.3.1 SE+PE+MP
63 pipeline using $k=65$ -mers, $t=65$, $q=3$, $e=3$, $E=0$, $c=3$, $m=30$, $p=0.9$, no scaffolding at
64 PopBubbles, $s=200$, $n=10$, overlap min=5 with scaffolding and join masking at simple
65 repeats, SimpleGraph $d=6$ and scaffolding, greedy MergePaths, $a=4$, and abyss-scaffold
66 min-gap=100. The SE stage used PE-short+medium+long, MP-short+long, the PE stage
67 was applied to PE-short+medium+long, and the MP stage was applied to MP-short+long.
68 The assembly was taken as the final scaffolds of nt length $\geq 130 = 2k$. Based on
69 alignments, scaffolds apparently consisting of PhiX, chrC, or chrM were removed.

70 Genome annotation revealed several nearly identical genomic contigs with nearly
71 identical fold coverage, which appear to be due to a failure of the assembler to collapse
72 identical contigs into one contig. In an effort to resolve this artifact from the assembler,
73 we performed all versus all BLASTn for each genomic contig against the whole genome
74 and removed contigs which contained a >95% threshold for query coverage and
75 nucleotide identity. This reduced the total number of contigs from 199,501 to 116,817
76 (41.3% reduction) and total genome size from 182,854,974bp to 161,759,242bp
77 (excluding the mitochondrial and chloroplast genomes).

78 Notation for contigs is in the form of gXXXXXX_YYYYY, where XXXXXX
79 gives contig length and YYYYY gives the approximate average coverage for that contig.
80 Contigs beginning with a 'g' are genomic sequences and contigs beginning with an 'r' are
81 mRNA sequences.

82

83 *DNA Bisulfite sequencing and analysis*

84 1 µg of *C. cryptica* nuclear DNA for bisulfite treatment was resuspended in 50 µl of
85 EB buffer (QIAGEN) and sonicated in AFA-fiber microTubes using a Covaris S2
86 machine (Duty Cycle = 10%; Intensity = 5; Cycles/Burst = 200; for 6 minutes) to obtain
87 100-300 bp fragments. The DNA was then subjected to End-Repair, A-tailing and
88 Adapter Ligation using Illumina TruSeq DNA Sample Prep kit v2 according to
89 manufacturer's instructions. The Adapter-ligated DNA was purified and size-selected
90 using AMPure XP beads. DNA was then bisulfite treated using EpiTect kit (QIAGEN)
91 using the following conversion protocol: 95°C 5min, 60°C 25min, 95°C 5min, 60°C
92 85min, 95°C 5min, 60°C 175min, 95°C 5min, 60°C 25min, 95°C 5min, 60°C 85min,

93 95°C 5min, 60°C 175min. Bisulfite-treated DNA was then desulphonated according to
94 manufacturer's protocol ("Small Amount of Fragmented DNA" variant) and DNA eluted
95 twice with EB. Converted DNA was amplified with MyTaq 2x mix (Bioline): 98°C 2
96 min; 12 cycles of 98°C 15 sec, 60°C 30 sec, 72°C 30 sec; 72°C 5 min. Amplified DNA
97 was diluted to 10 nM and sequenced using Illumina HiSeq2000 (100 single end reads).

98 Bisulfite converted reads were inspected for sequencing quality using FastQC 0.10.1.
99 Reads passing the Illumina quality filter ('PF' value equal to 1) were retained and aligned
100 to the genome assembly using BS-Seeker2 in local alignment mode with Bowtie2 as the
101 aligner [2]. For the purpose of this study, a 'methylated' base pair is defined as a cytosine
102 which has ≥ 4 methylated reads, similar to as described in [3]. Therefore an
103 'unmethylated' cytosine is that which has ≥ 4 unmethylated reads. Those cytosines
104 which do not have at least 4 aligned reads from the bisulfite sequencing are considered to
105 not have enough data sufficiently conclude whether that site is methylated or not. Genes
106 that are 'methylated' are those which are defined as having $\geq 50\%$ of callable CG sites
107 (the most common motif for methylation) containing a 'methylated' cytosine.
108 Unmethylated genes are $< 50\%$.

109 *RNA sequencing*

110 Total RNA was purified from cultures of *C. cryptica* in log-phase growth under
111 conditions of either silicon starvation or nitrogen starvation. For RNA isolation, 750mL
112 of liquid cell culture for each time point was harvested and treated with 20mg/mL
113 cycloheximide and concentrated by filtration. Cells were stored in -80°C prior to
114 extraction. Total RNA was extracted according to [4,5].

115 Five µg of total RNA per sample was treated with Turbo DNase (Ambion) for 30 min
116 at 37°C according to the manufacturer's instructions in order to remove any
117 contaminating DNA. The resulting RNA was purified by ethanol precipitation, and RNA
118 quality was evaluated on a BioAnalyzer RNA Nano kit (Agilent). RNAseq libraries were
119 prepared using the Illumina TruSeq mRNA Sample Prep kit (Illumina) according to
120 manufacturer's protocols (Rev. A). Sequencing was performed at the UCLA Broad Stem
121 Cell Research Center sequencing core on a HiSeq 2000 sequencer (Illumina) using a
122 mixture of 50+50 nt paired end reads and 100 nt single end reads. 11 libraries were
123 sequenced on a single lane each, 2 libraries were multiplexed onto a 1 lane. Pooled raw
124 reads were demultiplexed and all reads mapped to transcriptome data, with remaining
125 unmapped reads mapped to reference *Cyclotella* genome version cycCry0dot2 using
126 TopHat 2.0.4 allowing for two mismatches, reporting only unique mappings [6]. Bam
127 files were processed through HTSeq 0.5.3 using the "intersection-nonempty" method
128 which assigns a read to a gene only if the read overlaps with only one gene in its entirety.
129 Single-end and paired-end data were combined and all data was run through DESeq 1.8.3
130 to obtain FPKM counts [7]. A combination of 50+50 nt paired end reads and 100 nt
131 single end reads were pooled to facilitate accurate mapping of the genes.

132

133 *Genome Annotation*

134 Gene model predictions were generated from several pipelines as follows: (1)
135 FGENESH using the built-in diatom training set; (2) standalone AUGUSTUS using the
136 built-in '*Chlamydomonas reinhardtii*' training parameters; (3) standalone AUGUSTUS
137 using the 100 longest FGENESH predictions as a training set; (4) web-based

138 AUGUSTUS trained on the de-novo RNA assembly; and (5) MAKER with FGENESH,
139 AUGUSTUS, GeneMarkES analyses enabled [8-11]. All prediction software was run
140 using default settings except where noted. Several genes were selected where
141 intron/exon boundaries were well characterized in *T. pseudonana* and used to test the
142 accuracy of the gene model predictions. AUGUSTUS predictions from set (4) that
143 overlap MAKER predictions from set (5) constitute the 'high-confidence' collection of
144 gene predictions. For gene structure, it was determined that (4) more accurately
145 predicted start/stop sites and intron/exon boundaries. Gene set (4 and 5) were functionally
146 annotated [12].

147 Repetitive elements were identified using RepeatMasker 4.0.1 with RMBLASTN
148 2.2.27+, using the Bacillariophyta repeat library from RepBase and default settings.
149 Additional repeat masking by RepeatMasker was performed using a custom de-novo
150 library generated using RepeatModeler 1.0.7 with the NCBI BLAST engine.

151 The diatom genomes used in Figure 9 and S2, OrthoMCL, and RBH analyses are
152 *T. pseudonana* v3.0 [13], *P. tricornutum* v2.0 [14], *F. cylindrus* v1.0 [15], *P. multiseriata*
153 v1.0 [16], and *T. oceanica* v.3.0 (NCBI accession numbers JP288099-JP2977110,
154 <http://www.ncbi.nlm.nih.gov>)

155 For reciprocal best BLAST hit (RBH) analysis, gene models from diatom genomes
156 (listed above) were aligned using BLASTp 2.2.28+ [17], with an e-value cutoff score of
157 1e-5 and a query coverage of at least 70%. RBH pairs were detected using python script
158 [18].

159 Predicted proteins from *T. pseudonana* and *C. cryptica* genomes were evaluated for
160 phylogenetic relatedness to sequences in NCBI GenBank nr (accessed October 16, 2015)

161 using the DarkHorse program version 1.5 with a threshold filter setting of 0.1 [24].
162 BLASTP alignments to GenBank nr sequences were required to cover at least 70% of
163 total query length and have e-value scores of $1e^{-5}$ or better for inclusion in this analysis.

164 For phylogenetic analysis in Figure 9 and S2, and to further investigate proteins of
165 interest, amino acid sequences were aligned using MUSCLE with 10 maximum number
166 of iterations and default parameters [19]. Trees were generated using default parameters
167 in RAxML_GUI v1.3 for 100 iterations and visualized using FigTree v1.4.0 [20]. For
168 each tree shown, bootstrap values are listed and have been midpoint rooted.

169

170 *Subcellular Localization Prediction*

171 All open reading frames were analyzed using several computational tools for
172 predicting the likely location of the protein product within the cell. Nucpred [21] and
173 NetNES [22] provided estimations of nuclear localization for each putative protein.
174 PREDOTAR [23], PSORT [24], HECTAR [25], CELLO [26], PredAlgo [27], SignalP
175 3.0 [28] TargetP, ChloroP [29] and ASAFind [30] provided possible localizations to
176 mitochondria, chloroplast, endoplasmic reticulum, or plastid. The presence of N-terminal
177 signal peptides and transmembrane regions were assessed using PHOBIUS [31,32], the
178 SignalP 3.0 portion of TargetP and PredAlgo. Specific sequences and predicted cleavage
179 sites for signal peptides were taken from SignalP 3.0. All open reading frames from *C.*
180 *cryptica* were submitted to web-servers in an automated fashion using scripts for html or
181 webmail submission.

182 Methods for targeting predictions shown in Figure 4 are as follows: for plastid
183 targeting, all proteins with predicted positive ASAFind plastid targeting were surveyed for

184 proper cleavage site using SignalP 3.0 [28, 30]. Predicted SignalP 3.0 cleavage sites were
185 then defined by the guidelines addressed in Figure 5 of [33] and split into canonical
186 plastid (AF, GF, and SF cleavage sites), noncanonical plastid (AW, AY, AL, GW, GY,
187 GL, SW, SY, SL), periplastid and other (AH, AI, AM, AR, AE, AG, SH, SI, SM, SR, SE,
188 SG, GH, GI, GM, GR, GE, GG). Periplastid predicted cleavage sites which did not
189 contain a positive ChloroP prediction were then categorized as ER/secreted. Any negative
190 plastid ASAfind result but SignalP 3.0 positive with a predicted periplastid cleavage site,
191 and positive ChloroP were also classified as periplastid. ER/secreted proteins were then
192 defined as proteins with negative plastid ASAfind prediction, positive SignalP 3.0, with a
193 cleavage site not one that is specified in [33].

194 Mitochondrially-targeted proteins were classified according to any of the
195 following prediction combinations for HECTAR, Predotar, and TargetP (listed in
196 respective order): Type II, Mito, Mito; SigP, Mito, Mito; Mito, Plastid, Mito; Mito, Mito,
197 SigP; Mito, Mito, Mito; Mito, Mito, Plastid; Mito, Mito, no prediction; Mito, no
198 prediction, Mito; no prediction, Mito, Mito. MitoProt was also used for all predicted
199 proteins shown in Figure 5-8 [34]. All other proteins that did not fall into the above
200 criterion were classified as ‘cytosol and other.’

201

202 *Vector Construction and Diatom Transformation*

203 The vector utilizing the *C. cryptica* rpL41 promoter and terminator sequences was
204 assembled using the GeneArt® Seamless Cloning and Assembly Kit (Invitrogen), with a
205 Gateway™ vector (Invitrogen) as the backbone. The construction of the *T. pseudonana*
206 *fcp* [35] and nitrate reductase (NR) [36,37] vectors is described elsewhere.

207 Each vector was co-transformed with another vector expressing the *natI* gene
208 (received from N. Kroger, Germany), which confers resistance to the antibiotic
209 nourseothricin, under control of the acetyl coenzyme A carboxylase promoter. *C. cryptica*
210 was transformed using tungsten microparticle bombardment as described elsewhere
211 (Shrestha and Hildebrand, 2014), with the following changes: 1×10^7 cells in exponential
212 phase were spread onto artificial sea water (ASW) containing 1.5% Bacto Agar (Becton
213 Dickinson, USA) and no antibiotics [38]. Immediately after bombardment, 10ml ASW
214 was added to the plates, which were incubated in low light for 18 hours. Following the
215 incubation, cells were washed off the plates using the ASW they were incubated with,
216 and the entire volume was transferred to 125ml Erlenmyer flasks with 50ml ASW with
217 100 μ g/ml nourseothricin (clonNAT; Werner BioAgents, Germany). After 7 days of
218 growth with shaking, 10ml of the cultures were transferred to 125ml Erlenmeyer flasks
219 with fresh 50ml ASW plus 100 μ g/ml nourseothricin and grown to exponential phase. The
220 highest GFP expressors were selected using a sorting flow cytometer (Influx, Becton
221 Dickinson, USA), recovered in liquid ASW for 2 days, then plated on ASW agar plates
222 with 100 μ g/ml nourseothricin. Colonies were picked and transferred to 24 well plates,
223 each well containing 2 ml ASW with 100 μ g/ml nourseothricin.

224

225 *Assessment of Conditional Expression Using the Nitrate Reductase Promoter*

226 Three independent clones were grown to exponential phase in 24 well plates, as
227 described above. 2 μ l of culture was transferred to two new wells per clone. One of the
228 wells contained 2ml ASW, which would allow for expression of GFP under the NR
229 promoter. The other well contained 2ml modified ASW, in which ammonia replaced

230 nitrate as the nitrogen source, which would repress the expression of GFP under the NR
231 promoter [36]. The cultures were allowed to reach exponential phase and imaged using
232 Zeiss Axio Observer Z1 Inverted Microscope (Zeiss Axioscope, Carl Zeiss Microimaging
233 Inc., USA). The filter set for fluorescent imaging was Emission LP 515 nm for
234 chlorophyll autofluorescence, and Zeiss #38HE Excitation BP 470/40 nm, Dichromatic
235 mirror FT 495 nm, Emission BP 525/50 nm for GFP.

236

237

238

239

240

241

242 1. Jacobs JD, Ludwig JR, Hildebrand M, Kukel A, Feng T-Y, Ord RW, et al.
243 Characterization of two circular plasmids from the marine diatom *Cylindrotheca*
244 *fusiformis*: plasmids hybridize to chloroplast and nuclear DNA. *Molec. Gen. Genet.*
245 1992;233:302–10.

246 2. Guo W, Fiziev P, Yan W, Cokus S, Sun X, Zhang MQ, et al. BS-Seeker2: a versatile
247 aligning pipeline for bisulfite sequencing data. *BMC Genomics.* 2013;14:774.

248 3. Lopez DA, Hamaji T, Kropat J, De Hoff P, Morselli M, Rubbi L, et al. Dynamic
249 changes in the transcriptome and methylome of *Chlamydomonas reinhardtii* throughout
250 its life cycle. *plantphysiol.org. American Society of Plant Biologists;*
251 2015;169:00861.2015–743.

252 4. Smith SR, Glé C, Abbriano RM, Traller JC, Davis A, Trentacoste E, et al. Transcript
253 level coordination of carbon pathways during silicon starvation-induced lipid
254 accumulation in the diatom *Thalassiosira pseudonana*. *New Phytol.* 2016;210:810-904.

255 5. Hildebrand M, Dahlin K. Nitrate transporter genes from the diatom *Cylindrotheca*
256 *fusiformis* (Bacillariophyceae): mRNA levels controlled by nitrogen source and by the
257 cell cycle. *J. Phycol.* 2000;36:702-13.

258 6. Kim D, Pertea G, Trapnell C, Pimentel H, Kelley R. TopHat2: accurate alignment of
259 transcriptomes in the presence of insertions, deletions and gene fusions. *Genome Biol.*
260 2013;14:R36.

- 261 7. Love MI, Huber W, Anders S. Moderated estimation of fold change and dispersion for
262 RNA-seq data with DESeq2. *Genome Biol.* 2014;15:550.
- 263 8. Stanke M, Morgenstern B. AUGUSTUS: a web server for gene prediction in
264 eukaryotes that allows user-defined constraints. *Nucleic Acids Res.* 2005;33:W465–7.
- 265 9. Cantarel BL, Korf I, Robb SMC, Parra G, Ross E, Moore B, et al. MAKER: An easy-
266 to-use annotation pipeline designed for emerging model organism genomes. *Genome*
267 *Res.* 2007;18:188–96.
- 268 10. Salamov AA. Ab initio Gene Finding in Drosophila Genomic DNA. *Genome Res.*
269 2000;10:516–22.
- 270 11. Borodovsky M, Lomsadze A. Eukaryotic gene prediction using GeneMark.hmm-E
271 and GeneMark-ES. *Curr Protoc Bioinformatics.* 2011;Chapter 4:Unit4.6.1–10.
- 272 12. Lopez D, Casero D, Cokus SJ, Merchant SS, Pellegrini M. Algal Functional
273 Annotation Tool: a web-based analysis suite to functionally interpret large gene lists
274 using integrated annotation and expression data. *BMC Bioinformatics.* 2011;12:282.
- 275 13. Joint Genome Institute. <http://genome.jgi.doe.gov/Thaps3/Thaps3.home.html>
- 276 14. Joint Genome Institute. <http://genome.jgi.doe.gov/Phatr2/Phatr2.home.html>
- 277 15. Joint Genome Institute. <http://genome.jgi.doe.gov/Fracy1/Fracy1.home.html>
- 278 16. Joint Genome Institute. <http://genome.jgi.doe.gov/Psemu1/Psemu1.home.html>
- 279 17. Altschul SF, Gish W, Miller W, Myers EW. Basic local alignment search tool. *J. Mol.*
280 *Biol.* 1990;215:403-10.
- 281 18. Qin H. hongqin/Simple-reciprocal-best-blast-hit-pairs.
- 282 19. Edgar RC. MUSCLE: multiple sequence alignment with high accuracy and high
283 throughput. *Nucleic Acids Research.* 2004;32:1792–7.
- 284 20. Stamatakis A. RAxML-VI-HPC: maximum likelihood-based phylogenetic analyses
285 with thousands of taxa and mixed models. *Bioinformatics.* 2006;22:2688–90.
- 286 21. Brameier M, Krings A, MacCallum RM. NucPred Predicting nuclear localization of
287 proteins. *Bioinformatics.* 2007;23:1159–60.
- 288 22. La Cour T, Kierner L, Mølgaard A, Gupta R, Skriver K, Brunak S. Analysis and
289 prediction of leucine-rich nuclear export signals. *Protein Engineering Design and*
290 *Selection.* 2004;17:527–36.
- 291 23. Small I, Peeters N, Legeai F, Lurin C. Predotar: A tool for rapidly screening
292 proteomes for N-terminal targeting sequences. *Proteomics.* 2004;4:1581–90.

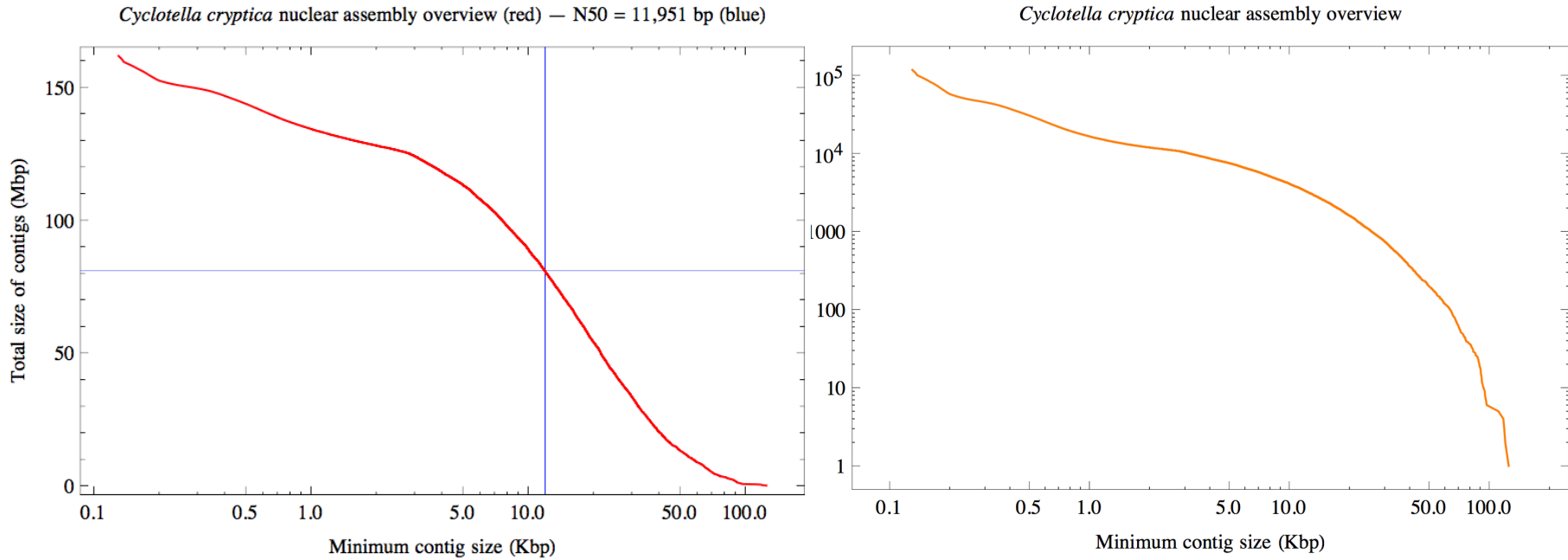
- 293 24. Horton P, Park KJ, Obayashi T, Fujita N, Harada H, Adams-Collier CJ, et al. WoLF
294 PSORT: protein localization predictor. *Nucleic Acids Res.* 2007;35:W585–7.
- 295 25. Gschloessl B, Guermeur Y, Cock JM. HECTAR: A method to predict subcellular
296 targeting in heterokonts. *BMC Bioinformatics.* 2008;9:393.
- 297 26. Yu C-S, Lin CJ, Hwang J-K. Predicting subcellular localization of proteins for Gram-
298 negative bacteria by support vector machines based on n-peptide compositions. *Protein*
299 *Science.* Cold Spring Harbor Laboratory Press; 2004;13:1402–6.
- 300 27. Tardif M, Atteia A, Specht M, Cogne G, Rolland N, Brugiere S, et al. PredAlgo: A
301 New Subcellular Localization Prediction Tool Dedicated to Green Algae. *Mol Biol Evol.*
302 2012;29:3625–39.
- 303 28. Dyrlov Bendtsen J, Nielsen H, Heijne von G, Brunak S. Improved Prediction of
304 Signal Peptides: SignalP 3.0. *J Mol Biol.* 2004;340:783–95.
- 305 29. Emanuelsson O, Brunak S, Heijne von G, Nielsen H. Locating proteins in the cell
306 using TargetP, SignalP and related tools. *Nat Protoc.* 2007;2:953–71.
- 307 30. Gruber A, Rocap G, Kroth PG, Armbrust EV, Mock T. Plastid proteome prediction
308 for diatoms and other algae with secondary plastids of the red lineage. *Plant J.*
309 2015;81:519–28.
- 310 31. Laws EA, Taguchi S, Hirata J, Pang L. Optimization of microalgal production in a
311 shallow outdoor flume. *Biotechnol. Bioeng.* 1988;32:140–7.
- 312 32. Käll L, Krogh A, Sonnhammer E. A Combined Transmembrane Topology and Signal
313 Peptide Prediction Method. *J Mol Biol.* 2004;338:1027–36.
- 314 33. Gruber A, Vugrinec S, Hempel F, Gould SB, Maier U-G, Kroth PG. Protein targeting
315 into complex diatom plastids: functional characterisation of a specific targeting motif.
316 *Plant Mol Biol.* 2007;64:519–30.
- 317 34. Claros MG, Vincens P. Computational method to predict mitochondrially imported
318 proteins and their targeting sequences. *Eur J Biochem.* 1996.
- 319 35. Shrestha RP, Hildebrand M. Evidence for a Regulatory Role of Diatom Silicon
320 Transporters in Cellular Silicon Responses. *Eukaryot Cell.* 2014;14:29–40.
- 321 36. Poulsen N, Chesley PM, Kröger N. Molecular genetic manipulation of the diatom
322 *Thalassiosira pseudonana* (Bacillariophyceae). *J. Phycol.* 2006;42:1059–65.
- 323 37. Trentacoste EM, Shrestha RP, Smith SR, Glé C, Hartmann AC, Hildebrand M, et al.
324 Metabolic engineering of lipid catabolism increases microalgal lipid accumulation
325 without compromising growth. *Proc Nat Acad Sci.* 2013;110:19748–53.

326 38. Darley WM, Volcani BE. Role of silicon in diatom metabolism. *Exp Cell Res.*
327 1969;58:334–42.

328

Figure S1: (a) *Cyclotella cryptica* nuclear assembly overview broken down by minimum contig size (Kbp) versus total Mbp of all contigs (left) and minimum contig size versus the total number of contigs (right) and (b) genomic sequencing data.

a.



b.

Genomic Libraries	Number of Raw Reads for Paired End Libraries				Percentage passing pairs				Percentage passing pairs after removal of pairs with 'N'
	Lane 1	Lane 2	Lane 3	Total Reads	Lane 1	Lane 2	Lane 3	Average	Average
Paired End Short	65270867	17592293		82863160	4.8	57		71.1	73.0
Paired End Medium	65333130	66235838		131568968	68.5	69.5		60.0	79.6
Paired End Long	69147985	69578501	65179466	203905952	27.8	34	65.6	42.5	57.9
Paired End Control	30301553				92.8				99.5
Mate Pair Short	142455072				96.9				98.9
Mate Pair Long	154107079				96.7				98.6

Supplementary table S1. Statistics from different gene model prediction pipelines. The pipelines are: (1) FGENESH Gene predictions, Diatom training set, (2) Augustus Gene predictions V1, *Chlamydomonas* training set, no RNAseq data, (3) Augustus Gene predictions V2, FGENESH100 training set, RNAseq data (4) Augustus Gene predictions V3, 'self' trained, RNAseq data (5) MAKER Gene predictions, (Augustus self trained + FGENESH + GeneMarkES). Details are presented in Supplementary Methods. Data presented includes all predicted models regardless of read counts from RNAseq data and prior to removing apparent duplicate contigs (Additional File 1: Supplementary Methods, Genome Library Construction and Sequencing).

	Gene Model Prediction Pipeline				
	CcFgenesh	CcAugustusV1	CcAugustusV2	CcAugustusV3	CcMAKERV1
Total Models	50,288	6,295	24,819	33,682	9,049
Average Model Length (bp)	1,561.8	926.1	1,746.2	1,265	1,999.7
Average Exons	3.72	1.22	2.65	1.95	3.69
Avg. Exon Length (bp)	247.4	115.8	561.5	585.6	457.6
Avg. # Introns	2.72	0.22	1.65	0.95	2.69
Avg. Intron Length (bp)	129.8	542	153.9	128.1	128.1

Table S2: Repeat sequences in *C. cryptica* identified using (a) RepBase data and (b) RepeatModeler Data.

b.

a.

Repeat sequences in *Cyclotella cryptica* using RepBase data

Sequences: 199501

total length: 182854974 bp (174198679 bp excl N/X-runs)

GC level: 43.01%

Bases masked: 7037708 bp (3.85 %)

	Number of elements*	Length occupied (bp)	Percentage of sequence
Retroelements	12264	4694900	2.57
SINEs:	0	0	0
Penelope	13	1650	0
LINES:	58	4854	0
CRE/SLACS	0	0	0
L2/CR1/Rex	0	0	0
R1/LOA/Jockey	0	0	0
R2/R4/NeSL	0	0	0
RTE/Bov-B	2	100	0
L1/CIN4	0	0	0
LTR elements:	12206	4690046	2.56
BEL/Pao	0	0	0
Ty1/Copia	2901	1432661	0.78
Gypsy/DIRS1	9305	3257385	1.78
Retroviral	0	0	0
DNA transposons	346	113716	0.06
hobo-Activator	0	0	0
Tc1-IS630-Pogo	0	0	0
En-Spm	0	0	0
MuDR-IS905	0	0	0
PiggyBac	2	103	0
Tourist/Harbinger	305	105959	0.06
Other (Mirage, P-element, Transib)	0	0	0
Rolling-circles	0	0	0
Unclassified:	28	6197	0
Total interspersed repeats:		4814813	2.63
Small RNA:	142	17166	0.01
Satellites:	0	0	0
Simple repeats:	32133	1928189	1.05
Low complexity:	3624	294614	0.16

Repeat sequences in *Cyclotella cryptica* using RepeatModeler data

Sequences: 199501

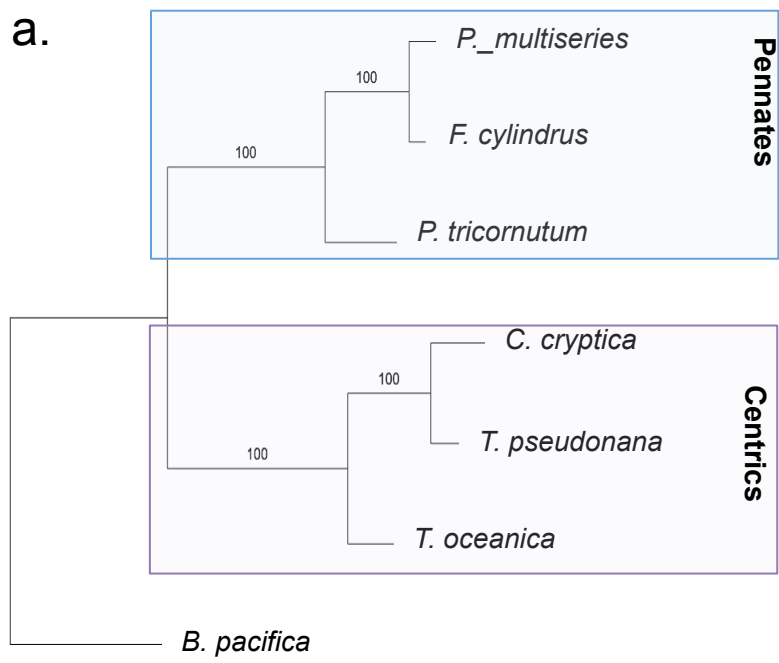
Total length: 182854974 bp (174198679 bp excl N/X-runs)

GC level: 43.01 %

Bases masked: 98288109 bp (53.75 %)

	Number of elements*	Length occupied (bp)	Percentage of sequence
SINEs:	0	0	0
ALUs	0	0	0
MIRs	0	0	0
LINES:	2626	1877047	1.03
LINE1	0	0	0
LINE2	0	0	0
L3/CR1	0	0	0
LTR elements:	43176	15802661	8.64
ERVL	0	0	0
ERVL-MaLRs	0	0	0
ERV_classI	0	0	0
ERV_classII	0	0	0
DNA elements:	15402	5899536	3.23
hAT-Charlie	0	0	0
TcMar-Tigger	155	44023	0.02
Unclassified:	314059	73067346	39.96
Total interspersed repeats:		96646590	52.85
Small RNA:	0	0	0
Satellites:	0	0	0
Simple repeats:	23628	1861243	1.02
Low complexity:	1672	129011	0.07

Figure S2: Phylogenetic comparison of diatom species with sequenced genomes. (a) 18S sequence comparison from [89], accession numbers are listed in Additional File 4 (b) Reciprocal best blast hits comparison. *C. cryptica* and *T. pseudonana* are the most similarly related centric diatoms with available genomic data.



b.

	Total Reciprocal BLAST Hits	Average % Identity
<i>C. cryptica/T. pseudonana</i>	5498	63.6
<i>C. cryptica/T. oceanica</i>	4443	56.4
<i>T. pseudonana/T. oceanica</i>	3592	59.2
<i>P. tricornutum/F. cylindrus</i>	7060	55.5
<i>P. tricornutum/P. multiseriis</i>	2878	54.2
<i>F. cylindrus/P. multiseriis</i>	7773	66.0

Figure S3: Per-cytosine fraction methylation. (a) 0 hour, silicon-replete sample (b) 48 hour, silicon-deplete sample. All sites shown have a read coverage greater than or equal to 4.

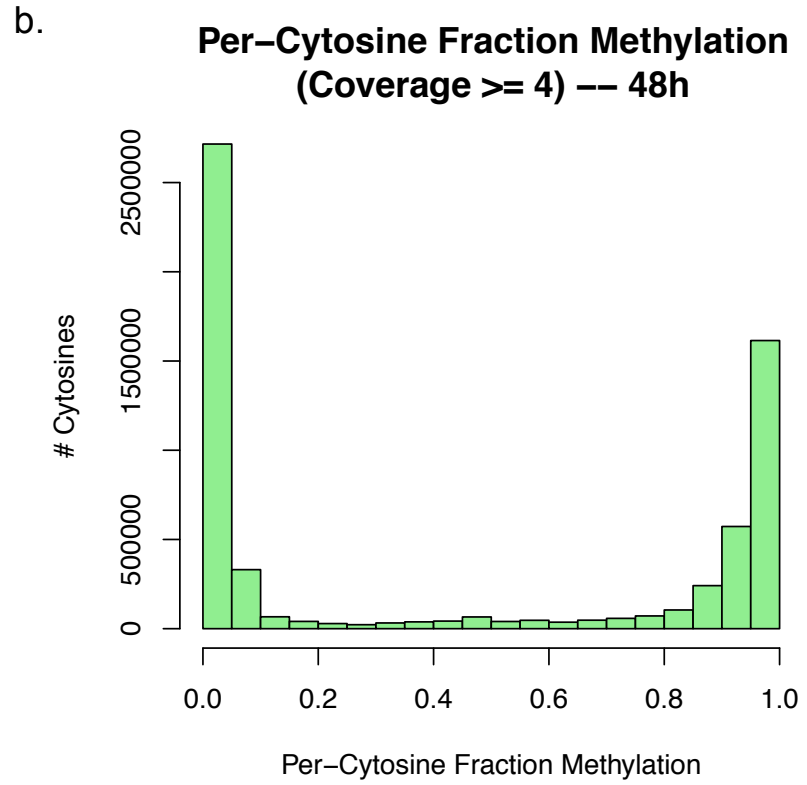
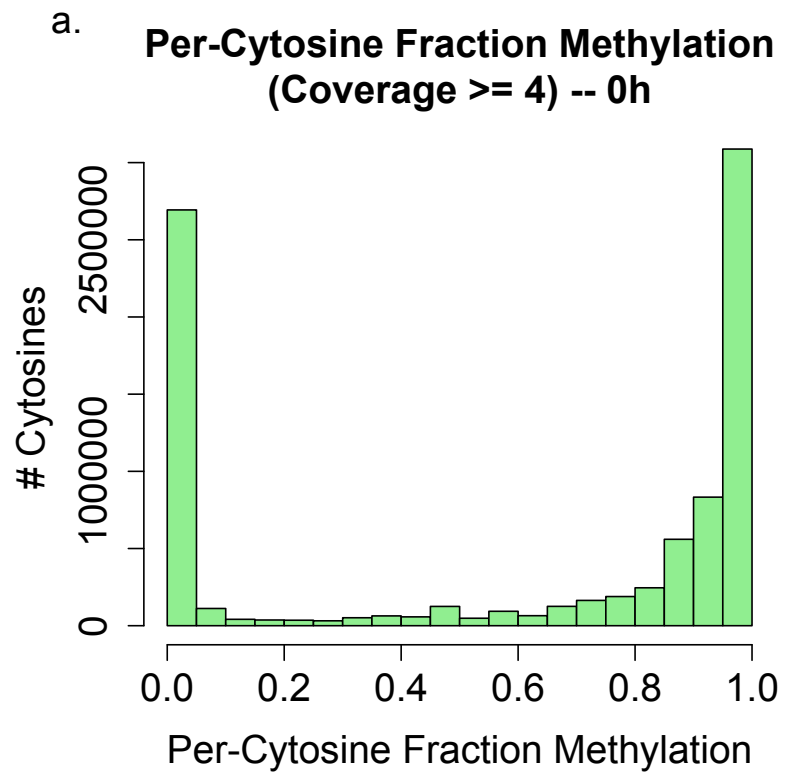


Figure S4: Per-site methylation differences between Silicon replete and deplete conditions. (a) Absolute value of the difference between 48h and 0h. (b) Slope between fraction methylation of genes in when comparing the two conditions is linear, outliers are apparent.

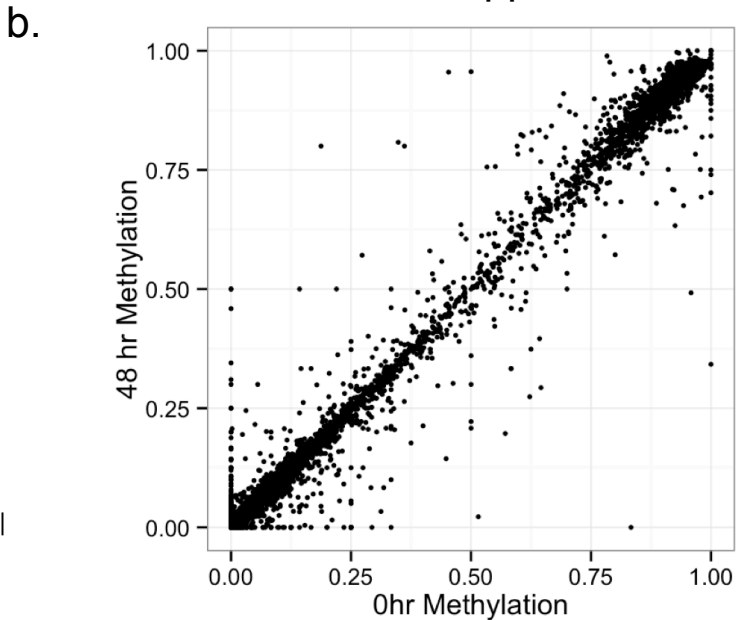
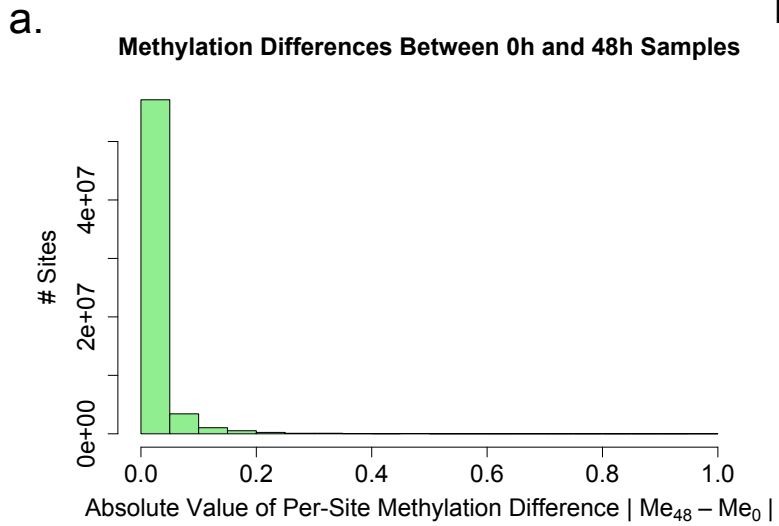


Figure S5: Per-site methylation differences between silicon replete and deplete conditions. (a) Histogram showing absolute value of the difference between 48h and 0h. (b) Scatter plot showing the slope between fraction methylation of genes in when comparing the two conditions is linear, outliers are apparent.

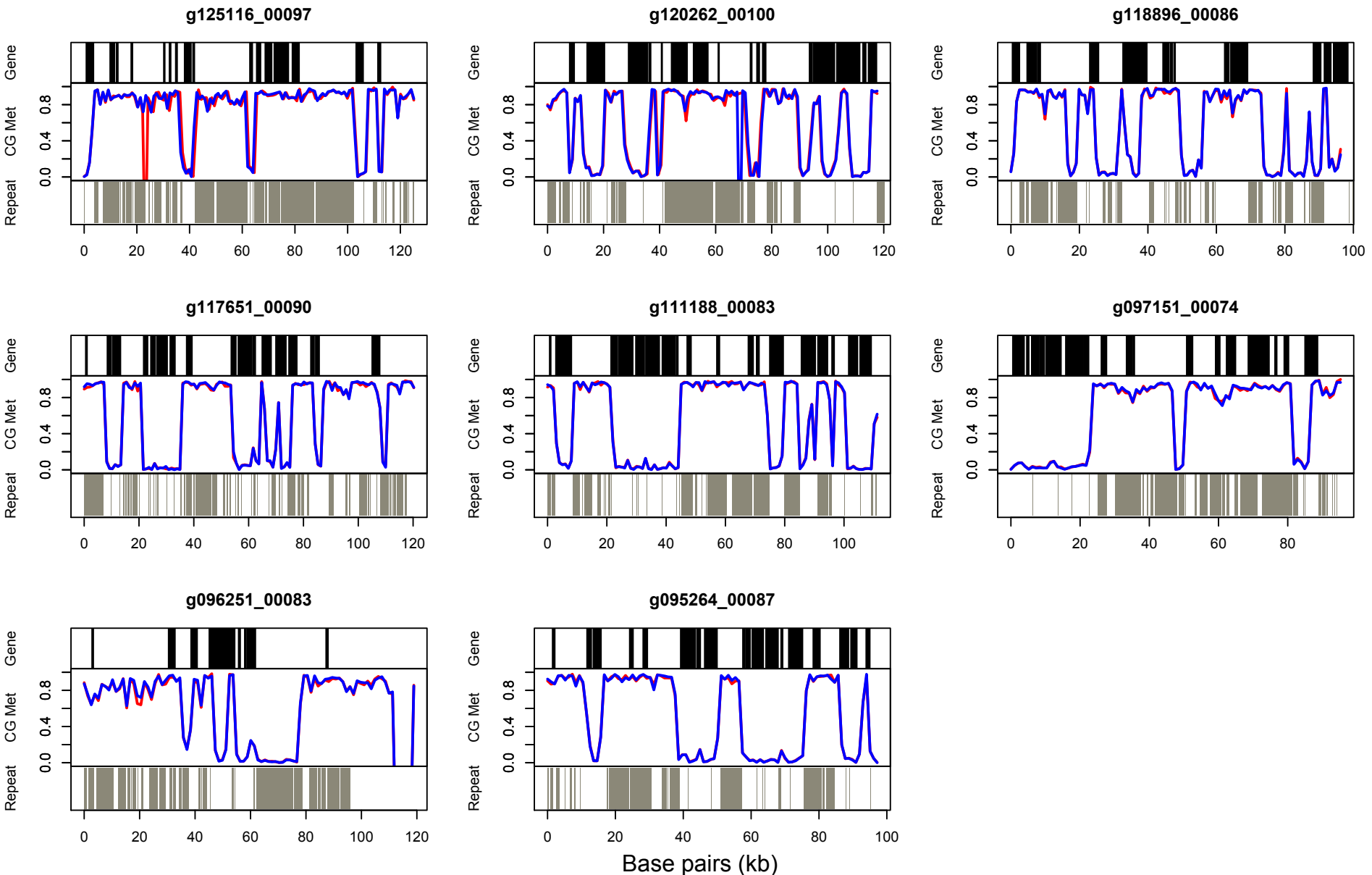


Figure S6: Binned repeats (a) and fraction methylation across gene body (b) in *C. cryptica*.

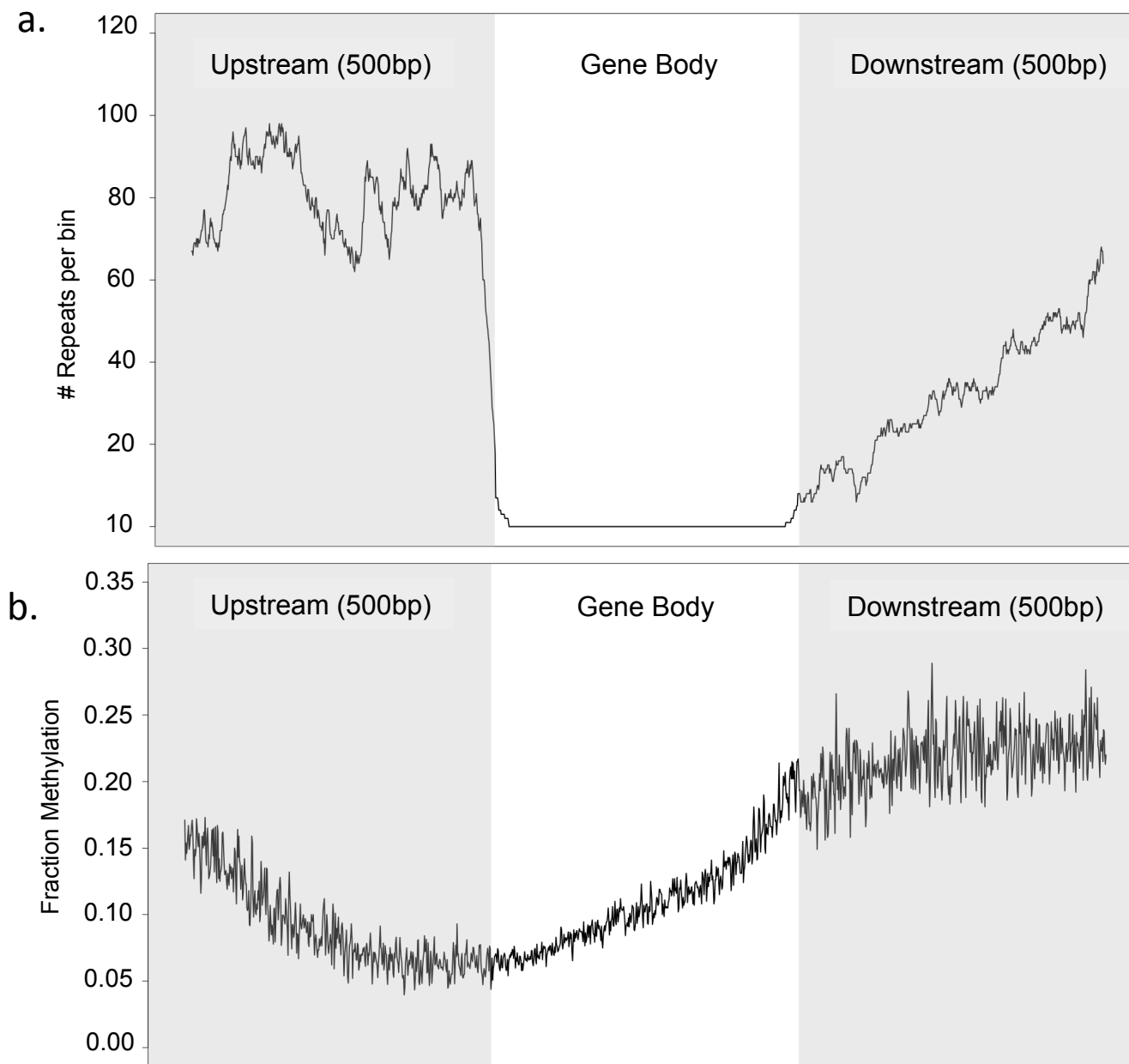


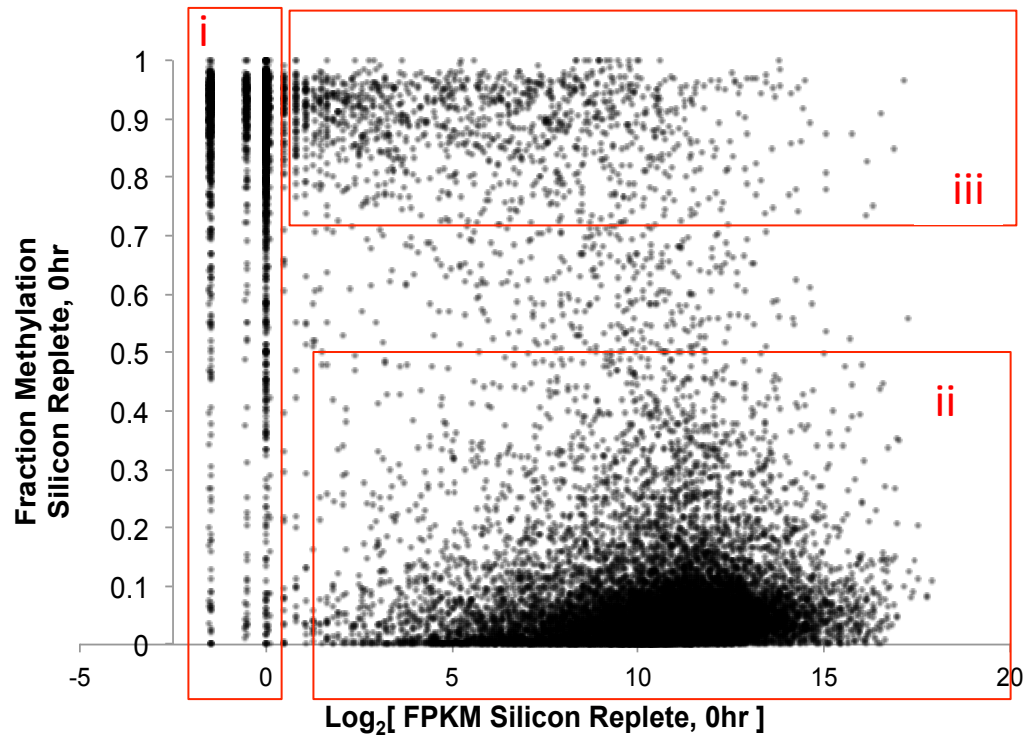
Table S3: Summary of gene methylation (AUGUSTUS V3 models) in both experimental conditions.

Silicon Replete 0hr					
	Count	Percent total of all genes	Percent total Excluding genes with insufficient coverage	Average Fraction Methylation	Average FPKM
Methylated genes	4170	20	22	0.87	536
Unmethylated genes	14866	70	78	0.07	4593
No Methylation Data	2085	10	-	ND	1767
Total genes	21121			0.24	3520
Silicon Deplete 48hr					
	Count	Percent total of all genes	Percent total Excluding genes with insufficient coverage	Average Fraction Methylation	Average FPKM
Methylated genes	2627	12	24	0.88	523
Unmethylated genes	8453	40	76	0.07	4589
No Methylation Data	10041	48	-	ND	3641
Total genes	21121			0.26	3408

	Methylated 48hr	Unmethylated 48hr
Methylated 0hr	2584	31
Unmethylated 0hr	17	8165

Figure S7: Gene methylation relative to gene expression. (a) 3 populations emerged (Red boxes i-iii) when comparing average fraction methylation to Log₂ FPKM. (b) Gene count binned according to FPKM and shaded according to methylation status. Line depicts the proportion of methylated genes per bin. Data shown is for silicon replete, 0 hour condition.

a.



b.

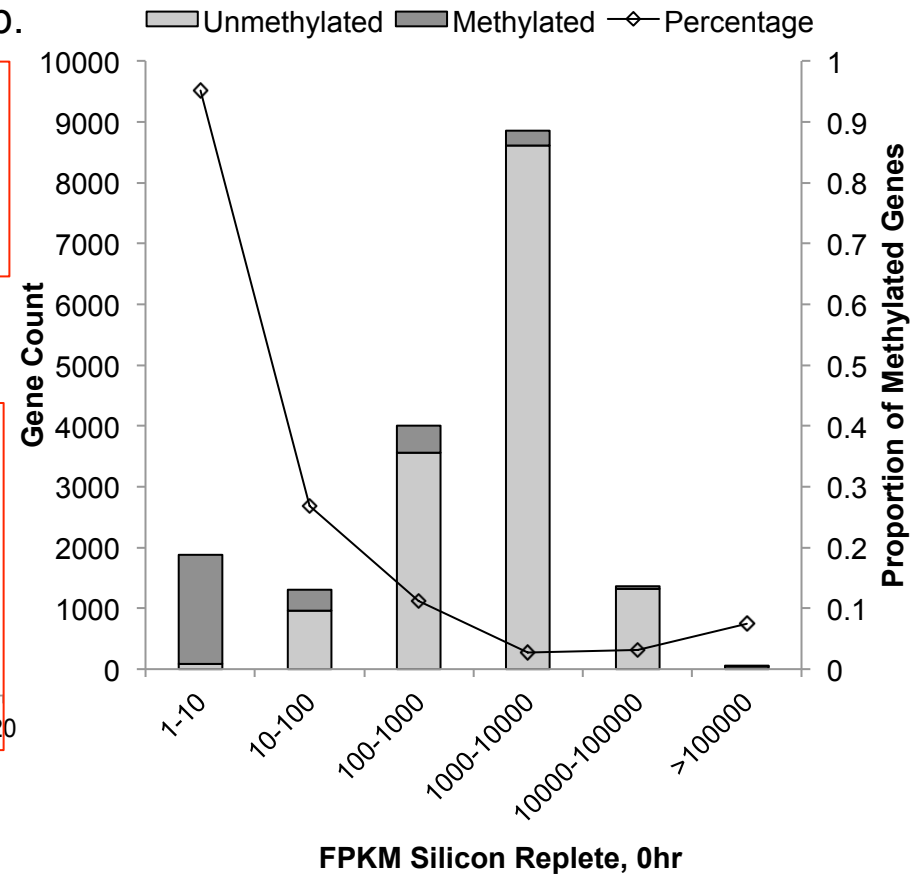


Figure S8: Vector map for rpL41 construct for *C. cryptica*.

